On the macrocyclization selectivity of *meta*-substituted diamines and dialdehydes: towards macrocycles with tunable functional peripheries

Gregor Klein[1,3] · Audrey Llevot[1,2] · Pia Löser[1] · Benjamin Bitterer[1] · Julian Helfferich[4] · Wolfgang Wenzel[4] · Christopher Barner-Kowollik[3] · Michael A. R. Meier[1]

Abstract

The efficient preparation of functional rigid and soluble macrocycles remains a challenge for synthetic chemists. Here, we exploit the thermodynamic control of dynamic covalent chemistry to investigate the influence of the monomer structure on the macrocyclization selectivity. A series of rigid cyclic hexamer has been synthesized by imine condensation of benzene building blocks, i.e. *meta*-substituted diamines and dialdehydes, templated by calcium(II) chloride. The monomers were designed to feature various additional functional groups either available for further post-cyclization modifications or acting as solubilizing groups. The cyclization selectivity was systematically investigated and optimized depending on the length of the applied solubilizing group and on the nature of the additional functional group. A selectivity up to 92% was reached for the macrocyclization exhibiting trifluoromethyl and bromine groups at the outer periphery and hydroxyl groups in the cavity.

Graphic abstract

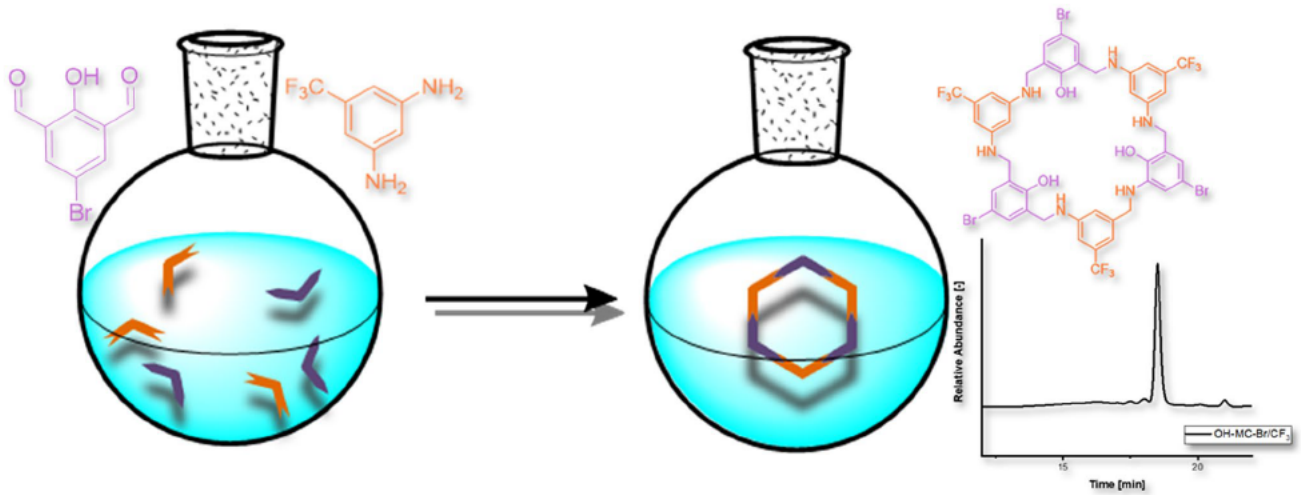

Keywords Macrocycle · Template · Schiff base · Selectivity

Introduction

Rigid macrocycles have gained increasing interest due to their unique structure and broad range of applications [1, 2]. Their architecture advantageously features planarity [3],

a defined cavity, precise positions of functional groups [4] and a conjugated system [5]. The presence of a defined cavity enables host–guest interactions, making macrocycles applicable as sensor materials [6] or artificial enzymes [3]. In material science, macrocycles can be used as building blocks to form supramolecular assemblies or three-dimensional porous structures that are suitable for catalysis [7] or artificial transmembrane transporters [8]. Furthermore, conjugated macrocycles are intensively studied for organic electronics [9], as their fully-conjugated structure provides unique electric, magnetic and optical properties [5].

Several synthetic approaches have been developed for the synthesis of rigid macrocycles [9]. Although kinetically controlled synthesis conditions offer a good possibility to design macrocycles, the employed stepwise syntheses generally result in low overall yields. As alternative, dynamic covalent chemistry, which relies on reversible covalent reactions, exhibits an error-correction capability that provides a thermodynamic control over the product composition [10–12]. Among the different reversible reactions fulfilling the requirements of dynamic covalent chemistry, alkyne, olefin and imine metatheses are commonly used for the construction of macrocycles in relatively high yields [13]. Initially, intensive research was devoted to the preparation of conjugated arylene-ethylene macrocycles by alkyne metathesis [14–17]. The high synthetic efficiency and selectivity of this pathway was directly correlated to the shape and angle persistency of the macrocycle containing rigid aromatic and alkyne groups. In contrast, imine and olefin metatheses resulted in macrocycles displaying more conformational freedom due to the double bond isomerism. Even if this increased flexibility led to a broader product distribution and to a decreased macrocycle selectivity, materials with novel functionalities and improved solubility could be produced [18, 19]. In order to expand the diversity of macrocyclic structures, all these chemistries were also combined to prepare unsymmetrical or heterosequenced macrocycles [20, 21]. One of the advantages of imine condensation (Schiff base reaction) lays in the possibility to use metal ions as templates to stabilize the macrocyclic structure [22, 23]. Indeed, the coordination bonds formed between the free electron pair of the nitrogen and the metal ion stabilizes the system and favors cyclization. Thus, the size of the macrocycle can be tuned by the radius of the metal ion [24]. This improved selectivity encouraged us to develop the herein discussed approach.

However, the solubility of rigid macrocycles is generally limited in common organic solvents. This drawback impedes their further functionalization and applications in electrochemistry or photochemistry, for instance. In order to overcome this issue, solubilizing groups, such as alkyl or alkoxyl chains, have been incorporated as side groups [25, 26]. Simulations enable the estimation of the cavity size and the determination of the position of the solubilizing groups [27–30]. However, the presence of solubilizing and of additional functional groups can impact the macrocyclization selectivity. Therefore, we report the synthesis of a series of benzene monomers constisting of *meta*-substituted dialdehydes and diamines featuring solubilizing and additional functional groups and investigate their suitability for the preparation of soluble functional macrocycles. The diamines display either a vinyl, ethyl or trifluoromethyl group as functional group (**X**). The dialdehydes bear hydroxyl, methoxyl, propoxyl or octoxyl groups as solubilizing groups (**OR**) and bromine or vinyl groups as functional groups (**Y**). The produced macrocycles were named **OR-MC-Y/X** (Scheme 1).

Results & discussion

Monomer synthesis

The functional dialdehyde **DAL-Y/OR** monomers were prepared in a three-step synthesis from 4-bromophenol

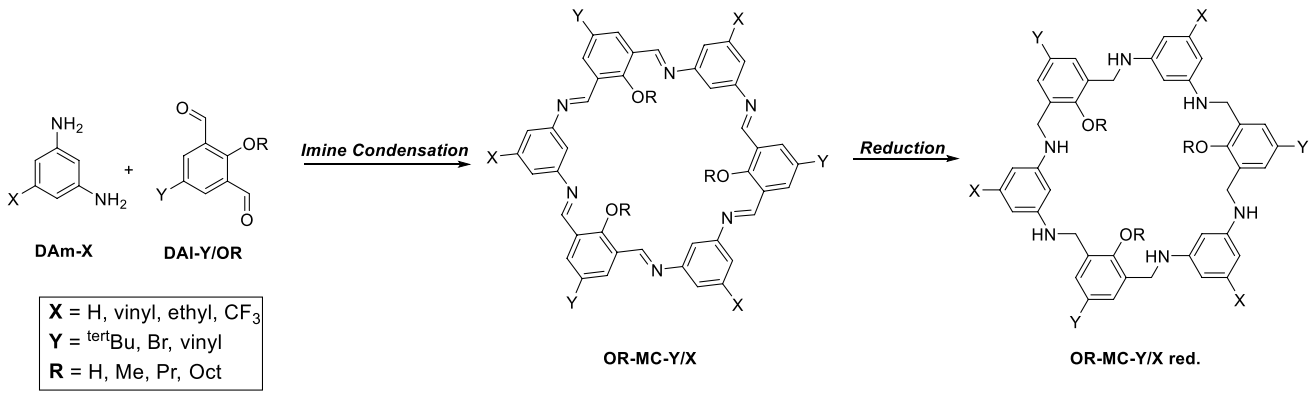

Scheme 1 Series of Schiff base reactions of diamines (**DAm-X**) and dialdehydes (**DAl-Y/OR**) to obtain imine macrocycles (**OR-MC-Y/X**) and the corresponding amine macrocycles (**OR-MC-Y/X red**) after reduction

(Scheme 2). In the first step, the aldehyde moieties were introduced via a Duff reaction on 4-bromophenol to obtain **DAl-OH/Br** in 57% yield [31, 32]. Subsequently, alkyl chains of different length (methyl, propyl, octyl) were incorporated as solubilizing groups by Williamson ether synthesis in 70, 61 and 31% yields, respectively. As an S_N2 reaction, the decreasing yield observed for an increasing alkyl halide chain length can be explained by steric hindrance. Finally, the vinyl moiety was introduced by a subsequent Suzuki coupling with potassium vinyl trifluoroborate in the presence of benzophenone as radical scavenger to prevent undesired polymerization. The three products (**DAl-OMe/Vinyl**, **DAl-OPr/Vinyl** and **DAl-OOct/Vinyl**) were obtained in similar yields ranging from 61 to 73% [33]. **DAl-OH/^{tert}Bu** (4-tertbutyl-2,6-diformylphenol), which was commercially available, was methylated by Williamson ether synthesis to produce **DAl-OMe/^{tert}Bu** in 88% yield. This synthetic approach provided a library of eight different aldehyde monomers carrying either a hydroxyl group or alkyl chains of different length as solubilizing groups and a bromine or a vinyl group as additional functional groups.

The diamine monomers **DAm-X** were synthesized in a two-step procedure (Scheme 3a). First, the vinyl functionality was introduced to 1-iodo-3,5-dinitrobenzene by a Suzuki coupling in 85% yield. Afterwards, using tin(II) chloride, the nitroso groups were reduced to the corresponding amines, without affecting the vinyl group, resulting in **DAm-Vinyl** with a 90% yield. Alternatively, 1,3-dinitro-5-vinylbenzene was hydrogenated in presence of palladium on charcoal to obtain **DAm-Ethyl** in 92% yield. Both diamine monomers were stored under Ar in a fridge to prevent a degradation. Furthermore, commercially available *m*-phenylenediamine (**DAm-H**) and 5-(trifluoromethyl)benzene-1,3-diamine (**DAm-CF$_3$**) were directly used monomers (Scheme 3b).

Investigation of the macrocyclization conditions

The optimal reaction conditions for macrocyclization via imine condensation were investigated employing *m*-phenylenediamine (**DAm-H**) and 5-(*tert*-butyl)-2-methoxyisophthalaldehyde (**DAl-OMe/^{tert}Bu**) as model monomers. The reactions were performed in methanol under reflux. After the reaction, the reduction of the imine bonds to the corresponding amines is required in order to freeze the equilibrium. The soluble products were directly hydrogenated and analyzed. The precipitate formed during the reaction was filtered off and analyzed as obtained or after hydrogenation in order to increase its solubility in common

Scheme 2 Synthesis of the dialdehyde monomer library

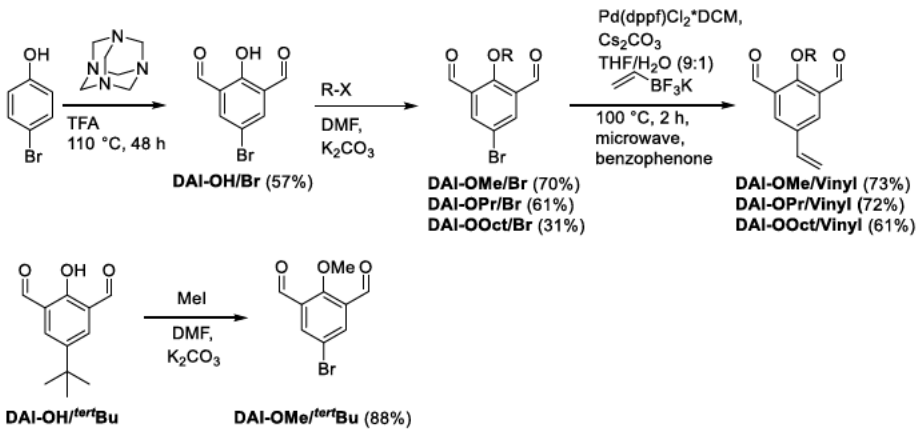

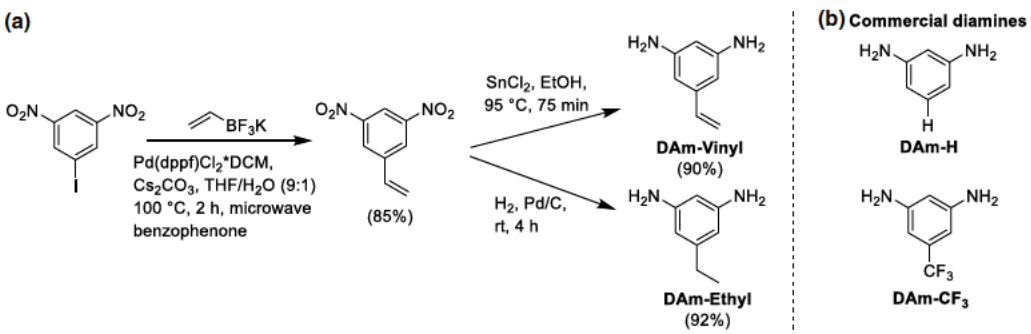

Scheme 3 **a** Synthesis of the diamine monomer library, **b** commercially available diamines used in this work

organic solvents. The product composition was determined by nuclear magnetic resonance spectroscopy (NMR) and by size-exclusion chromatography coupled to electronspray ionization mass spectrometry (SEC–ESI–MS). The influence of different reaction parameters such as solvent, catalyst and template species on the selectivity was examined. The first reaction was performed with one equivalent of each monomer for 6 h and without catalyst. This reaction did not lead to the formation of a precipitate. A mixture of monomers, dimers, trimers and macrocycle with a very low selectivity was observed in solution (see SI Fig. 22). The addition of an acid catalyst, such as HBr, and an elongation of the reaction time did not improve the reaction selectivity (see SI Fig. 22). When $CaCl_2$ was added as template, a product precipitated. The SEC chromatogram of the hydrogenated precipitate (Fig. 1a) exhibits a main peak at around 21.5 min. The mass observed for this peak corresponds to the desired macrocycle **DAl-OMe/*tert*Bu red** ($m/z(M^- + H^+) = 991.1172$; $m/z_{calc.} = 991{,}1181$; $\Delta m/z = 0.0009$) (Fig. 1b). The broad low intense peak observed at lower retention times reveals the presence of oligomers with higher molar masses. The ^{1}H NMR of the precipitate, which was soluble in benzene-d_6, displays the presence of all the characteristic peaks of the targeted macrocycle and especially the peak of the CH of the imine at 9.20 ppm (Fig. 2a). After hydrogenation, the imine signal disappeared and new peaks at 5.54 ppm and 4.12 ppm corresponding to the amine protons and the CH_2 in α-position were observed (Fig. 2b).

In order to improve the yield (25%) and selectivity (46%) of the precipitated macrocycle, several metal ions with different atomic radii were screened. The macrocycle precipitated from the reaction mixture when magnesium and calcium chlorides were used. Similar yields (around 25%) were reached after 4 h indicating that these ions have an adequate ionic radius (respectively 0.98 and 0.65 Å) to fit in the cavity of the macrocycle and favor its formation.

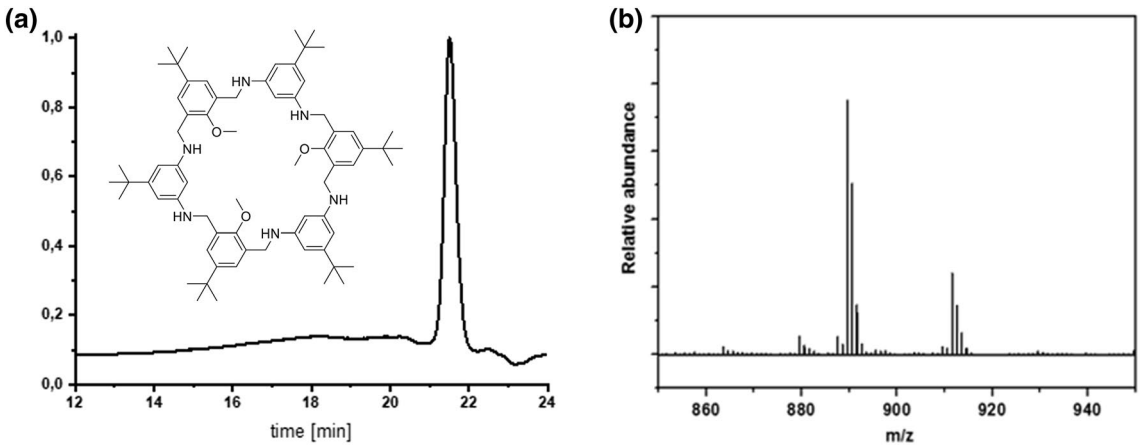

Fig. 1 **a** SEC trace of **OMe-MC-^{tert}Bu/H red**, **b** mass spectrum of **OMe-MC-^{tert}Bu/H red**

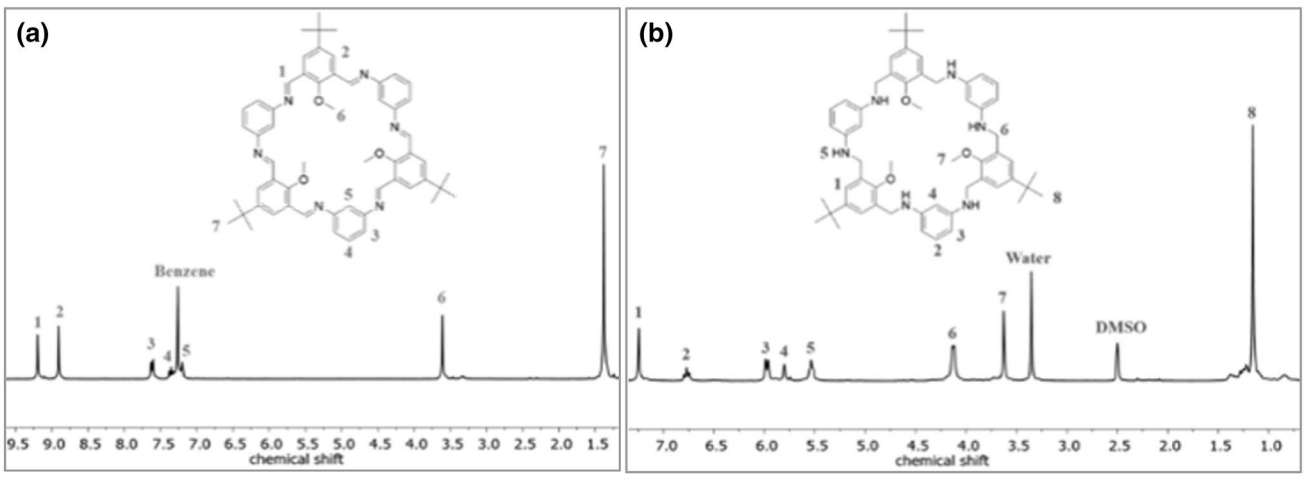

Fig. 2 ^{1}H-NMR spectrum of **OMe-MC-^{tert}Bu/H** (**a**) and **OMe-MC-^{tert}Bu/H red** (**b**)

Barium, which has an ionic radius of 1.35 Å, did not show any template effect. Finally, the replacement of methanol by dichloromethane or ethanol did not improve the selectivity.

Synthesis of functional macrocycles

After optimizing the reaction conditions on commercially available monomers, the synthesis of a series of functional macrocycles was investigated. The functional monomers described in the first section were combined in order to prepare a library of macrocycles with different side chains. All reactions were carried out under the same conditions: in methanol, under argon atmosphere, with a $CaCl_2$ template, unless otherwise mentioned. The yield, solubility and selectivity of the different monomer combinations were compared. In most cases, during the imine condensation, a precipitate containing the macrocyclic hexamer and other compounds, such as linear oligomers of high molar mass or other cyclic species was formed. The yield of precipitate was calculated considering the molar mass of the macrocycle including the presence of one Ca^{2+} and two Cl^- ions in its center to compare the different batches. Upon reduction, in a methanol/THF mixture (1:1) in presence of sodium borohydride, the solubilization of the precipitate was observed. The efficiency of the solubilization, which is directly related to the reduction efficiency, depends on the product structures. In some cases, the addition of $NaBH_4$ or THF and the extension of the reaction time was necessary to complete the solubilization. After extraction of the soluble part with chloroform, the reduction yield was calculated considering the molar mass of the reduced macrocycles without Ca^{2+}. The selectivity of the macrocyclization was calculated from SEC–ESI data; the peak displaying the mass of the macrocycle was identified on the chromatogram and its area integrated and compared to the total area. The non-isolated macrocycle yield was calculated by multiplication of the weighted yield after both the imine condensation and reduction step and the selectivity (Table 1).

Influence of the solubilizing group chain length

In a first series, **DAm-H** was combined with the different dialdehyde monomers. The reaction time required for the formation of the precipitate depended on the structure of the dialdehyde. Indeed, the product precipitated within few minutes or one hour when **DAl-OH/Br** and **DAl-OMe/Br** were used as dialdehyde comonomers, respectively. After 6 h of reaction time, the yields of precipitate were around 80% in both cases (see Table 1 SI). After a similar reaction time, the combination of **DAm-H** with **Dal-OPr/Br** and **Dal-OOct/Br** led to clear or slightly turbid reaction mixtures, respectively. Therefore, the reaction times for the last two monomers were extended to 13 h in order to reach a precipitate yield over 80%. The precipitates of all macrocycles were insoluble in common organic solvents. During the reduction of **OR-MC-Br/H**, the solubilization of all precipitates was observed, except for **Oct-MC-Br/H**. In this case, due to an increased solubility, longer oligomers, which might remain insoluble even after reduction, can be formed. Although, **OPr-MC-Br/H**, **OMe-MC-Br/H** and **OH-MC-Br/H** were soluble at the end of the reduction step, after work-up and evaporation of the solvent, a low solubility in common solvents, impeded their full characterization. A strong π–π stacking might explain the phenomenon.

The rest of the experiments were performed with diamines featuring an additional functional group, which might prevent π–π stacking, increases the solubility, thus enabling the estimation by SEC (Fig. 3).

DAm-CF_3 was combined with dialdehydes featuring solubilizing groups of different length. The reaction of **DAm-CF_3** with **DAl-OH/Br** resulted in the formation of a precipitate in a 77% yield. After reduction (quantitative yield), the peak at 17.88 min on the SEC–ESI chromatogram was identified as the macrocycle **OH-MC-Br/CF_3 red** ($m/z(M^- + H^+) = 1117.0319$; $m/z_{calc.} = 1117.0333$; $\Delta m/z = 0.0014$) (Figs. 3 and 4). A selectivity of 93% and a yield of non-isolated macrocycle of 72% were calculated. The small shoulder at 15.96 min is characteristic of oligomers with a higher molar mass. The ^{1}H-NMR spectrum of the reduced precipitate confirmed the macrocycle structure by displaying all the characteristic peaks of **OH-MC-Br/CF_3 red,** but unassigned impurities were present in the aliphatic region. In the optimization study, we only showed the crucial role of the template on the methylated monomer. However, in literature, some authors also reported the favorable influence of H-bond on the imine macrocycle formation [34, 35]. In order to clarify the template effect on monomers carrying OH groups, the same reaction was performed without template. Under these conditions, a precipitate was formed in a similar yield of 73%, but after reduction (quantitative yield), a decreased macrocycle selectivity of 49% was observed, thus underlining the role of the template. As expected from the optimization experiments, the attempt to form **OMe-MC-Br/CF_3** without template did not lead to precipitation, which is explained by the absence of H bonds to favor the cyclization. When $CaCl_2$ was added, a significantly lower precipitation yield (44%) and lower selectivity (43%) compared to the reaction with **DAl-OH/Br** was observed, revealing a lower but still existing impact of the template effect. The peak at 17.82 min on the SEC–ESI chromatogram was identified as **OMe-MC-Br/CF_3 red** ($m/z(M^- + H^+) = 1159.0790$; $m/z_{calc.} = 1159.0803$; $\Delta m/z = 0.0013$) (Fig. 3). Furthermore, the macrocycles with one, two and three remaining imine bonds were found ($m/z(M^- + H^+) = 1157.0657$; $m/z_{calc.} = 1157.0646$; $\Delta m/z = 0.0011$, $m/z(M^- + Na^+) = 1177.0535$;

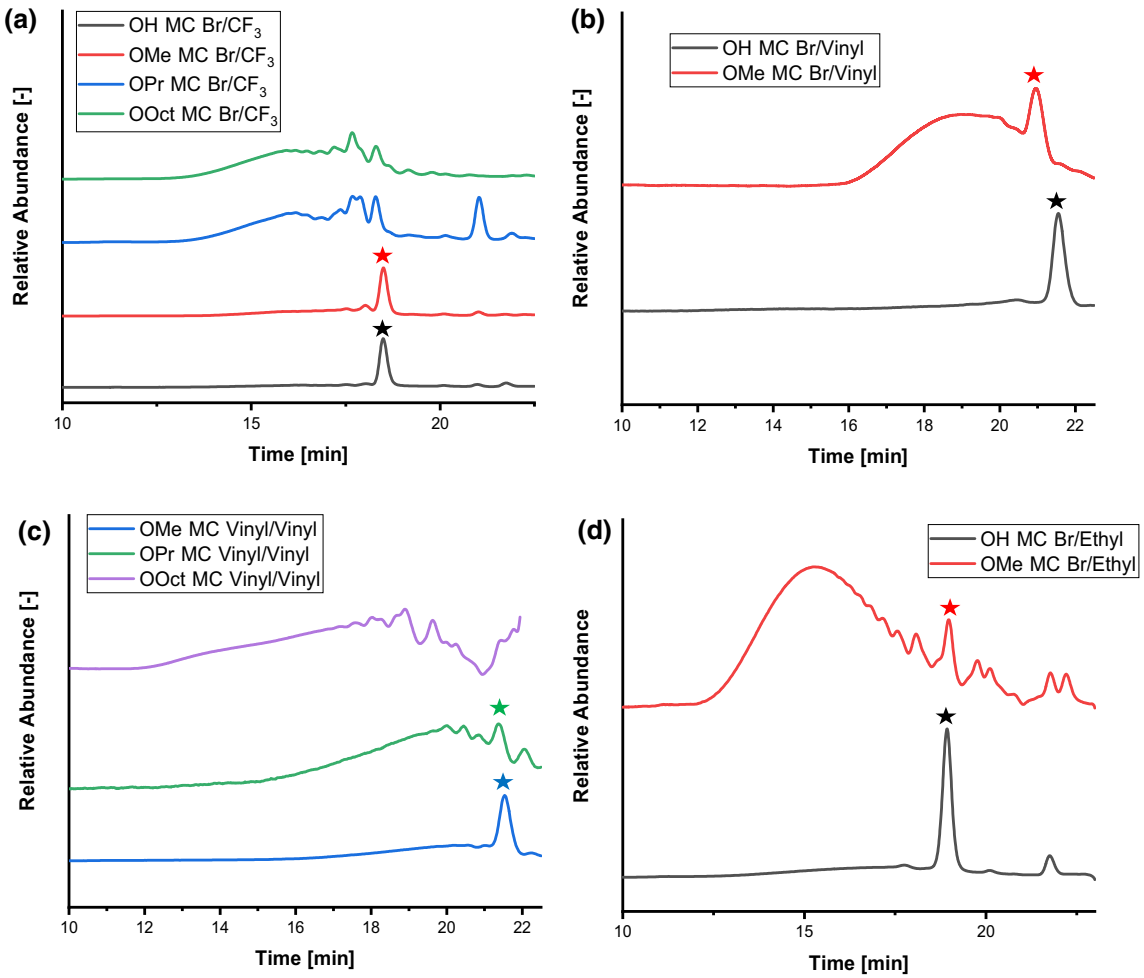

Fig. 3 **a** SEC traces **OH-MC-Br/CF$_3$**, **OMe-MC-Br/CF$_3$**, **OPr-MC-Br/CF$_3$** and **OOct-MC-Br/CF$_3$**, **b** SEC traces **OH-MC-Br/Vinyl**, **OMe-MC-Br/Vinyl**, **c** SEC traces **OMe-MC-Vinyl/Vinyl** and **OPr-MC-Vinyl/vinyl**, **d** SEC traces **OH-MC-Br/Ethyl** and **OMe-MC-Br/Ethyl**. The stars indicate the SEC peak corresponding to the macrocycle (determined from SEC–ESI)

$m/z_{calc.} = 1177.031$; $\Delta m/z = 0.0225$ and $m/z(M^- + Na^+) = 1175.0577$; $m/z_{calc.} = 1175.0153$; $\Delta m/z = 0.0424$), indicating incomplete hydrogenation, probably due to low solubility. When the length of the solubilizing group increased to a propyl group (**DAl-OPr/Br**), the precipitation yield continued decreasing to 20%. However, an increase of the yield was observed for the reaction with **DAl-OOct/Br.** This could be explained by the formation of longer oligomer chains due to an increased solubility and a lower influence of the template effect. No selectivity value was extracted from the SEC–ESI for **OPr-MC-Br/CF$_3$ red** and **OOct-MC-Br/CF$_3$ red**, as no adequate mass for the macrocycle was found. The chromatogram showed the presence of a majority oligomers with a higher molar mass.

A similar trend was observed for the macrocycles **MC-Br/Vinyl** prepared from **DAm-Vinyl** and different dialdehydes. The highest yield of precipitate (76%) and selectivity (86%) was reached for the **OH-MC-Br/Vinyl red** macrocycle. In the SEC chromatogram, a single, intense peak at 17.70 min with a small shoulder at 16.69 min. was observed. The peak at 17.70 min was identified as **OH-MC-Br/Vinyl red** ($m/z(M^- + H^+) = 991.1172$; $m/z_{calc.} = 991,1181$; $\Delta m/z = 0.0009$) by SEC–ESI (Figs. 3 and 4). The ^{1}H-NMR spectrum of the reduced precipitate confirmed the macrocycle structure by displaying all the characteristic peaks, but unassigned side products were present in the aliphatic region and could not be removed by chromatography. As for **MC-Br/CF$_3$**, introducing solubilizing groups favored the formation of longer linear oligomers and resulted in a lower macrocycle selectivity. A non-isolated macrocycle yield of only 5% was reached for **OMe-MC-Br/Vinyl red.** On the SEC–ESI, the peak at 21.0 min was identified as **OMe-MC-Br/Vinyl red** ($m/z(M^- + H^+) = 1055.1249$; $m/z_{calc.} = 1055.1471$; $\Delta m/z = 0.0222$).

The macrocycle **OH-MC-Vinyl/Vinyl** could not be synthesized, as it would require the reaction of **DAm-Vinyl** with

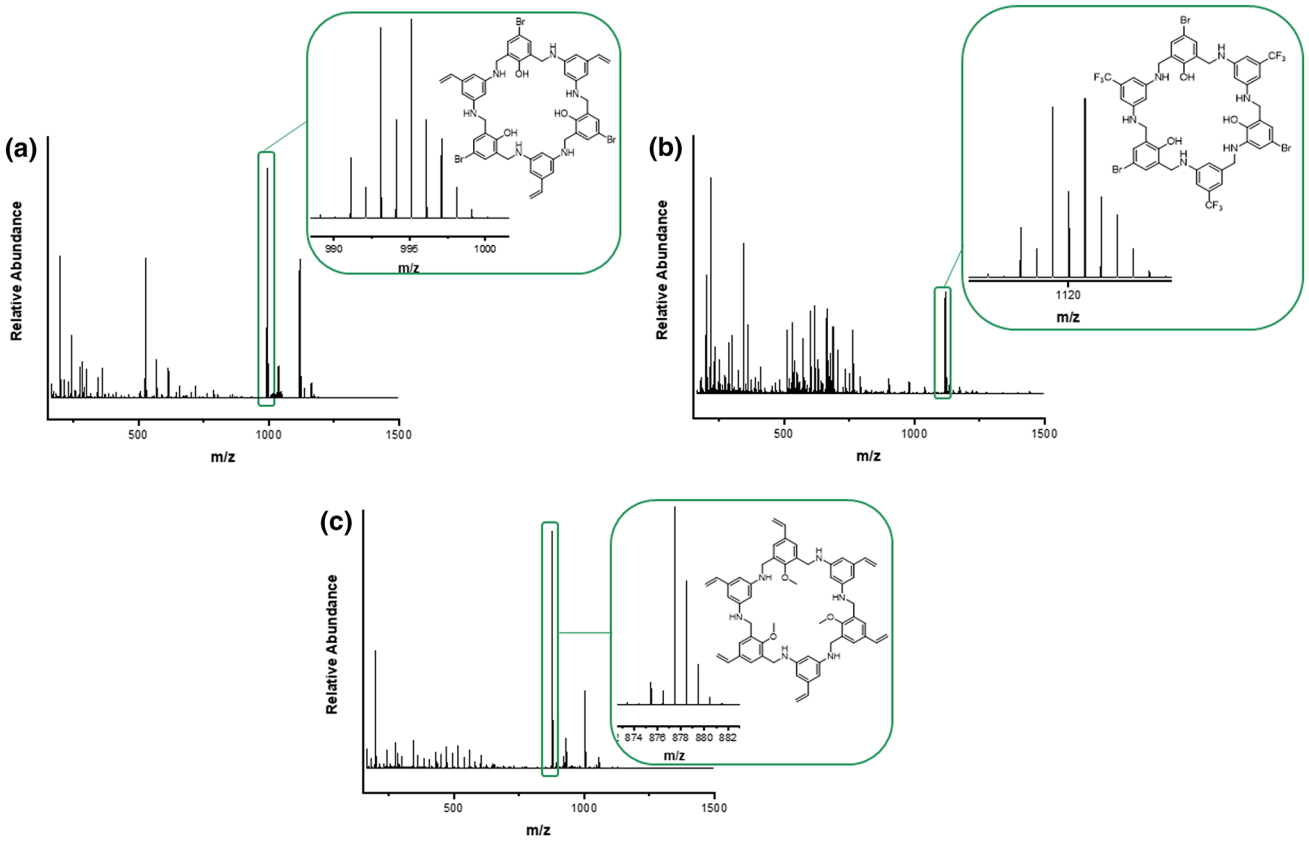

Fig. 4 Mass spectra of **OH-MC-Br/Vinyl red** (**a**), **OH-MC-Br/CF_3 red** (**b**), **OMe-MC-Vinyl/Vinyl red** (**c**)

Table 1 Overview of results of synthesis of macrocycles by imine condensation

Entry	Macrocycle	Yield of precipitate (%)	Yield of red (%)	Selectivity (%)	Non-isolated macrocycle yield (%)
1	**OH-MC-Br/CF_3**	77	Quant.	93	72
2	**OMe-MC-Br/CF_3**	44	Quant.	43	19
3	**OPr-MC-Br/CF_3**	20	94	–	–
4	**OOct-MC-Br/CF_3**	60	Quant.	–	–
5	**OH-MC-Br/Vinyl**	76	94	86	61
6	**OMe-MC-Br/Vinyl**	48	54	20	5
7	**OMe-MC-Vinyl/Vinyl**	36	43	36	6
8	**OPr-MC-Vinyl/Vinyl**	62	68	12	5
9	**OH-MC-Br/Ethyl**	77	92	62	44
10	**OMe-MC-Br/Ethyl**	83	82	6	4

Reaction conditions: Imine condensation: **DAm-X** (1 eq.), **DAl-Y/OR** (1 eq.) and $CaCl_2$ (1 eq.) in methanol ($c_{DAL\text{-}Y/OR}$ = 0.006 mol/L) under Ar atmosphere, 80 °C and stirred for respective time. Reduction: Precipitate suspended in mixture of methanol/THF (1:1) ($c_{precipitate}$ = 0.079 mol/L) and $NaBH_4$ (20 eq.) at room temperature for respective time

Calculations: The yield of precipitate was calculated considering the molar mass of the macrocycle including the presence of one Ca^{2+} and two Cl^- ions. The selectivity was calculated from SEC–ESI data by integration of the peak identified as the macrocycle and the total area. The non-isolated macrocycle yield was calculated by multiplication of the weighted yield after both the imine condensation and reduction step and the selectivity

DAl-OH/Vinyl that was not obtained as a pure monomer. Indeed, after the Duff reaction, the dialdehyde bearing the free OH group was used in a Heck and Suzuki coupling. The Heck coupling was unsuccessful and the Suzuki coupling led to a mixture of product and impurities, which were difficult to remove. **OMe-MC-Vinyl/Vinyl red** was synthesized with an overall low non-isolated macrocycle yield (6%), despite a correct selectivity of 36%. The peak at 17.53 min on the SEC–ESI chromatogram was identified as the macrocycle **OMe-MC-Vinyl/Vinyl red** ($m/z(M^- + H^+) = 877.4770$; $m/z_{calc.} = 877.4805$; $\Delta m/z = 0.0035$) (Figs. 3 and 4). The use of **OPr-DAl-Vinyl/Vinyl** as monomer led to the formation of a broad distribution of products according to the SEC–ESI. The peak at 17.57 min. could be identified as **OPr-MC-Vinyl/Vinyl red** ($m/z(M^- + H^+) = 961.5719$; $m/z_{calc.} = 961.5744$; $\Delta m/z = 0.0025$). Further linear oligomers were detected: the linear tetramer at 17.80 min, the linear pentamer with the aldehyde end groups at 17.30 min, the linear hexamer at 17.05 min, the linear heptamer with aldehyde end groups at 16.71 min and the linear octamer at 16.54 min.

In summary, in all cases, macrocycles were obtained with the highest yield employing monomers featuring free OH groups. Even if H-bonds increased the macrocycle stability, the addition of a template favored the cyclization reaction. Alkylation of the hydroxyl groups to increase the macrocycle solubility led to a decrease of macrocycle selectivity. Indeed, the template effect is reduced due to the steric hindrance inside the cavity. As a result of a lower template effect and increased solubility of the linear oligomers, longer oligomer chains precipitated out of the solution.

DFT calculations were conducted in order to calculate the cavity size and investigate the influence of solubilizing groups on the structure of the macrocycles. After the optimization of the structure, the energy of the macrocycles ("ground state energy" in Table 2) was compared to the single-point energy of the planar configuration ("energy of planar configuration" in Table 2) in order to assess the planarity of the macrocycles.

The minimized conformations showed that small solubilizing moieties, such as methoxy groups direct into the cycle plane (Fig. 5a) and longer alkyl chains, such as propoxyl groups, alternatively point out above and below the plane of the ring (Fig. 5b). The simulations indicate that the macrocycles are not fully planar, with energy differences ranging from 21.90 to 36.92 kJ/mol. The reduction of the ΔE with increasing the solubilizing group length indicates that the planar structure is more favorable for macrocycles with shorter substituents. Overall the simulations indicate that the macrocycles are slightly twisted but remain close to the planar conformation (Fig. 5).

The size of the cavity of the macrocycle can be estimated by calculation of the solvent accessible surface for a range of solvent radii. The radius of the intramolecular cavity of the macrocycles featuring, respectively, methoxy and propoxy sidegroups are 1.63 Å and 1.32 Å.

Influence of the functional group

With the objective to synthesize functional macrocycles, the monomers were designed to feature functional groups that could serve for post-cyclization modifications. **DAm-CF_3** was used as diamine to prepare macrocycles carrying on their periphery a trifluoromethyl group allowing post-functionalization. The fluorides can be exchanged to carbons with organoaluminium reagents [36], carboxylic acids can be obtained via hydrolysis with sulfuric acid [37] and various esters via alcoholysis in presence of an alcohol [38], which could be a method to integrate polyethylene glycol as molecular branches to the macrocycle. The trifluoromethyl group can also undergo a catalytic benzylation or alkylation [39]. Employing **DAm-Vinyl** as diamine monomer led to the formation of macrocycles with vinyl groups at the outer rim making post-modifications by olefin metathesis or thiol-ene addition possible for instance [40]. Employing **DAl-Br** as dialdehyde monomer resulted in the design of macrocycles with Br groups at the periphery, thus enabling post-modifications such as cross-coupling reactions or nucleophilic substitutions [41]. Additionally, the combination of diamines and dialdehydes featuring different functionalities provide macrocycles with anchor points for orthogonal modifications. The presence of these functional groups also influences the solubility of the produced macrocycles as well as the selectivity of the macrocyclization, parameters that must be considered.

As already discussed, the use of **DAm-H** resulted, after the work up and evaporation of the solvent, in a product with a low solubility in common solvents a due to a strong π–π stacking. After storage for a certain time, **OH-MC-Br/Vinyl red, OOct-MC-Br/Vinyl red, OMe-MC-Vinyl/Vinyl red, OPr-MC-Vinyl/Vinyl red** (see SI Figs. 26–33) were not soluble in organic solvent. In these cases a radical polymerization of the vinyl groups resulting in an insoluble

Table 2 Comparison of the DFT energies of the ground state and planar configuration for macrocycles with different solubilizing groups

	Ground state energy (a.u.)	Energy of planar configuration (a.u.)	ΔE (a.u.)	ΔE (kJ/mol)	Cavity size (Å)
OMe-MC-Vinyl/Vinyl	− 2754.9575	− 2754.9492	− 0.0083	− 21.90	1.63
OPr-MC-Vinyl/Vinyl	− 2990.8548	− 2990.8408	− 0.014	− 36.92	1.32

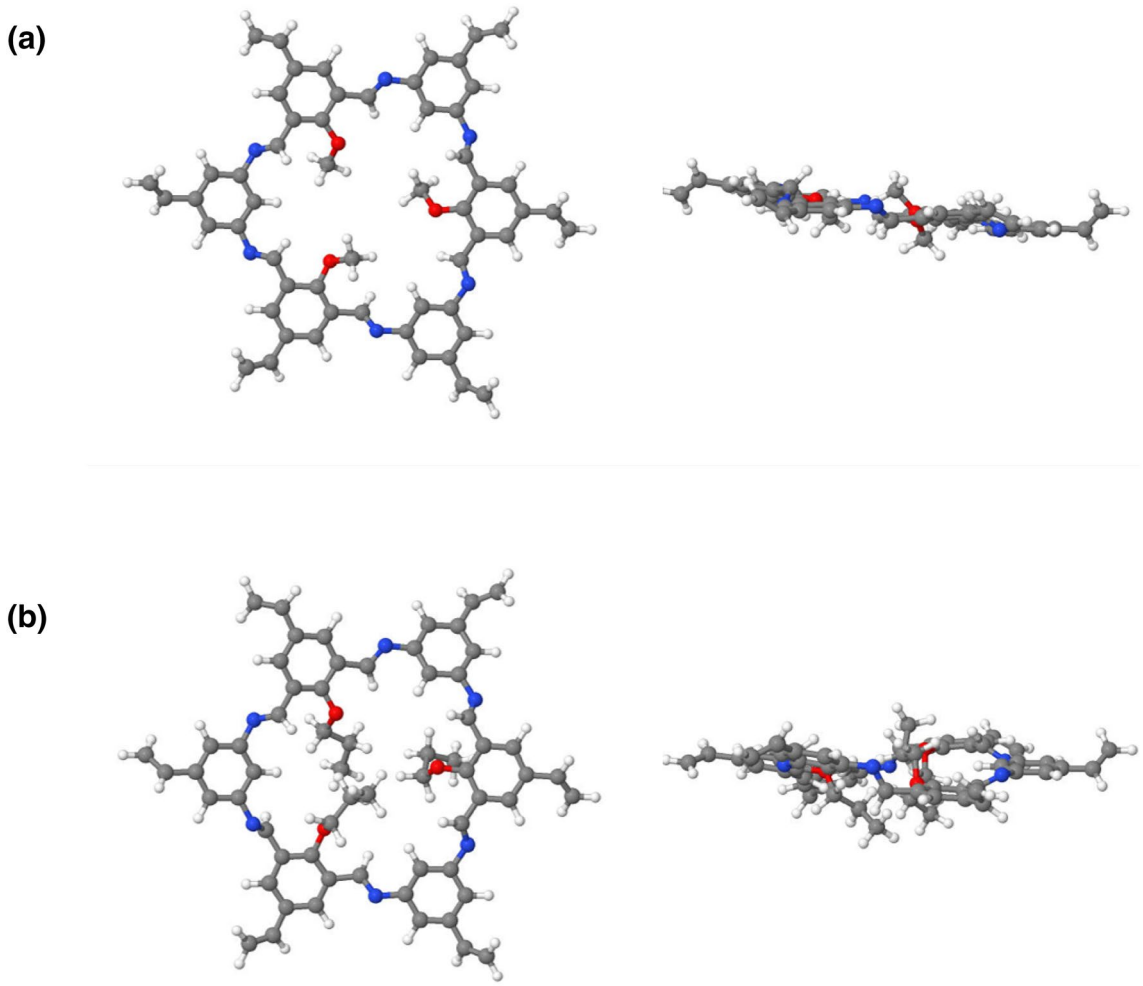

Fig. 5 Illustration of the DFT optimized configurations of the macrocycles **OMe-MC-Vinyl/Vinyl** (**a**), **OPr-MC-Vinyl/Vinyl** (**b**)

network, could occur due to light or temperature [42]. In order to prevent a radical polymerization of the double bond, the reaction was carried out in the presence of the radical scavenger *p*-benzoquinon. No improvement was observed, thus supporting the π–π stacking interaction hypothesis in this case as well.

The substitution of one of the functional group by an ethyl moiety was done in order to increase the solubility of the final macrocycle, prevent the π–π stacking and do not allow radical polymerization. According to the SEC–ESI analysis, **OH-MC-Br/Ethyl red** ($m/z(M^- + H^+) = 997.1640$; $m/z_{calc.} = 997.1651$; $\Delta m/z = 0.0011$) (Fig. 3) was obtained with a high selectivity (62%) as indicated by the intense peak at 18.20 min. In the mass spectrum, further macrocycles with remaining imine bonds were detected indicating that the reduction was not complete. The transformation of one imine bond is enough to break the fully-conjugated system and increase the solubility. However, the non-isolated yield of this macrocycle (44%) is lower compared to **OH-MC-Br/CF_3 red** (72%) and **OH-MC-Br/Vinyl red** (61%). This drop can be attributed to the enhanced solubility induced by the alkyl chain.

Conclusion

In this work, we have investigated synthetic pathways for the preparation of soluble macrocycles exhibiting peripheral functional groups. First, novel diamine and dialdehyde monomers were produced from aromatic compounds. This library of monomers featured methoxyl, propoxyl or octoxyl groups as solubilizing groups and bromine, vinyl or trifluoromethyl groups as functional groups. DFT calculations indicated that the configurations of the macrocycles remain almost planar, with just a slight twist. Optimization experiments underlined the favorable impact of adding a salt template on the macrocyclization formation. As a result, macrocycles featuring short solubilizing groups (methoxyl) in the cavity are formed with a higher selectivity. Moreover, the presence of free hydroxyl groups enables the formation

of hydrogen bonds that increase the macrocycle selectivity. The nature of the peripheral functional group also influences the reaction. The systematic approach reported in this study underlines the influence of key parameters, such as the monomer solubility, steric hindrance and the use of a template, on macrocyclization by imine condensation.

Analytics and equipment

Nuclear magnetic resonance (NMR) spectroscopy

^{1}H- and ^{13}C-NMR spectra were recorded on Bruker AVANCE DPK spectrometers operating at 300 MHz for ^{1}H-NMR and 75 MHz for ^{13}C-NMR and on Bruker AVANCE DRX with 400 MHz for ^{1}H-NMR and 100 MHz for ^{13}C-NMR. ^{1}H-NMR spectra were reported in parts per million (ppm) relative to the solvent signal. ^{13}C-NMR spectra were reported in ppm relative to the central line of the solvent signal. All measurements were performed at room temperature. The signal patterns were abbreviated in the following way: s = singlet, d = doublet, t = triplet, q = quartet, dd = doublet of doublets, dt = doublet of triplets, ddt = doublet of doublet of triplets, dtd = doublet of triplet o doublets, m = multiplet, br = broad.

Mass spectrometry (MS)

The samples were measured by fast atom bombardment mass spectrometry (FAB-MS) on a FINNIGAN MAT 95 instrument. Molecular fragments were specified as mass/charge ratio (*m/z)*. The protonated molecular ion was abbreviated as $[M+H]^{+}$.

Gas chromatography-mass spectrometry (GC–MS) (Electron ionization) chromatograms were recorded using a Varian 431 GC instrument with a capillary column Factor-FourTM VF-5 ms (30 m × 0.25 mm × 0.25 µm) and a Varian 210 ion trap mass detector. Scans were performed from 40 to 650 *m/z* at rate of 1.0 scan/s. The oven temperature program was: initial temperature 95 °C, held for 1 min, heated up at 15 °C per min to 200 °C, the temperature was held for 2 min., heated up at 15 °C per min to 325 °C, the temperature was held for 5 min. The temperature of the injector transfer line temperature was set to 250 °C. Measurements were performed in split–split mode (split ratio 50:1) using helium as the carrier gas (flow rate 1.0 mL per min).

Size exclusion chromatography (SEC)

The linear and cyclic oligomers were characterized on two systems:

The first system was a Shimadzu LC-20AD system equipped with a DGU-20A3R degassing unit, SIL-20A autosampler, RID-20A refractive index detector (24 °C), CBM-20A communications bus module and a Varian Pro Star column oven Model 510, operating at 40 °C. For separation, two SDV 3 µm linear S columns (8 × 300 mm) and a guard column (8 × 50 mm) were used. Detection was done by a differential refractive index detector operating in THF (flow rate 1.0 mL per min). For calibration linear poly(methylmethacrylate) standards (Agilent) ranging from 875 Da to 1677 kDa were used.

All runs were characterized on a Varian-SEC-LC gel permeation chromatography (SEC) system equipped with a LC-290 pump (Varian), refractive index detector (24 °C), PL AS RT SEC-autosampler (Polymer laboratories) and a Varian Pro Star column oven Model 510, operating at 40 °C. For separation, two PLgel 5 µm Mixed-d columns (8 × 300 mm) and a guard column (8 × 50 mm) were used. Detection was done by a refractive index detector operating in THF (flow rate 1.0 mL per min).

Size exclusion chromatography–electrospray ionization (SEC–ESI)

Spectra were recorded on a Q Exactive (Orbitrap) mass spectrometer (Thermo Fisher Scientific, San Jose, CA, USA) equipped with an HESI II probe. The instrument was calibrated in the *m/z* range 74–1822 using premixed calibration solutions (Thermo Scientific). A constant spray voltage of 4.6 kV, a dimensionless sheath gas of eight, and a dimensionless auxiliary gas flow rate of two were applied. The capillary temperature and the S-lens RF level were set to 320 °C and 62.0, respectively. The Q Exactive was coupled to a UltiMate 3000 UHPLC System (Dionex, Sunnyvale, CA, USA) consisting of a pump (LPG 3400SD), an autosampler (WPS 3000TSL), and a thermostated column department (TCC 3000SD). Separation was performed on two mixed bed size exclusion chromatography columns (Polymer Laboratories, Mesopore 250 × 4.6 mm, particle diameter 3 µm) with precolumn (Mesopore 50 × 4.6 mm) operating at 30 °C using THF at a flow rate of 0.30 mL per min was used as eluent. The mass spectrometer was coupled to the column in parallel to (an UV-Detector (VWD 3400 RS), and) a RI-detector (RefractoMax520, ERC, Japan) in a setup described earlier.[55] 0.27 mL per min of the eluent were directed through the RI-detector and 30 µL per min infused into the electrospray source after postcolumn addition of a 100 µM solution of sodium iodide in methanol at 20 µL per min by a micro-flow HPLC syringe pump (Teledyne ISCO, Model 100DM). A 20 µL aliquot of a polymer solution with a concentration of 2 mg/mL was injected into the HPLC system.

Solvents and reagents

HPLC grade solvents of chloroform (Fisher Chemicals), dichloromethane (DCM) (Fisher Chemicals), dimethylformamide (DMF) (Fisher Chemicals), ethanol (EtOH) (Fisher Chemicals), methanol (MeOH) (VWR), triethylamine (NEt_3), tetrahydrofuran (THF) (VWR) and toluene (99.7%, Bernd Kraft) were used. Water was deionized by passing through columns packed with ion exchange resins. As solvents for NMR spectroscopy, the following deuterated solvents were used: benzene-d_6 (99.8%, EuroIsotop), chloroform-d (99.8%, EuroIsotop), methanol-d_4 (99.8%, EuroIsotop) and THF-d_8 (99.8%, EuroIsotop).

The following chemicals were used as received: *p*-Benzoquinone (98%, Merck), [1,1′-bis(diphenylphosphino) ferrocene] dichloropalladium(II) complex with dichloromethane ($PdCl_2(dppf)CH_2Cl_2$) (ChemPur Feinchemikalien), *p*-bromophenol (99%, Sigma Aldrich), 1-bromopropane (99.0%, Acros), calcium chloride (Roth, 94%), Celite (pore volume 0.02–0.1 mm, Merck), cesium carbonate (Cs_2CO_3) (fluorochem), 2,6-di-*tert*-butyl-4-methyloxylphenol (99.8%, Acros), 3,5-dinitroaniline (97%, Sigma Aldrich), 1-iodo-3,5-dinitrobenzene (99%, abcr), hexamethylentetramine (Merck), 37% hydrochloride acid (analytic grade, Fisher Chemicals), methyl iodide (VWR), octyl bromide (99%, Sigma Aldrich), palladium on activated charcoal (Pd/C) (10% Pd base, Aldrich), potassium carbonate (Sigma Aldrich), potassium hydroxide (85%, Riedel de Haën), potassium vinyltrifluoroborate (95%, Ark Pharm. Inc.), sodium borohydride ($NaBH_4$) (98%, abcr), sodium sulfate (Na_2SO_4) (pure, Bernd Kraft), tin(II)chloride ($SnCl_2$) (Acros, anhydrous, 98%), trifluoracetic acid (TFA) (Acros 99%), 5-(trifluoromethyl)-1,3-phenylenediamine (98%, Aldrich), 1,3,5-trimethoxybenzene (99% Acros), trimethylsilylacetylene (98%, abcr GmbH) tri-*tert*-butylphosphonium tetrafluoroborate (tBu_3PHBF_4, 99%, abcr GmbH).

High-pressure laboratory reactor

Reactions with ethylene and hydrogen were carried out in a high-pressure laboratory reactor (highpreactorTM) BR-100 of the company Berghof equipped with grease-free valves and connections.

Microwave reactor

Microwave assisted syntheses were performed in a CEM EXPLORER 12 HYBRID microwave reactor using dynamic program at 150 W, 100 °C for 1 or 2 h. The reaction mixture was stirred with a magnetic stir bar at high speed in a 35 mL glass vessel sealed with a PTFE rubber band.

Simulation method

The structures of the macrocycles were assessed with density functional theory (DFT) as implemented in the NWCHEM[cite] code, using the generalized gradient approximation (GGA)with the hybrid B3LYP exchange–correlation functional. The calculations were performed with the 6-31G* basis set. In order to assess the effect of the exchange–correlation functional and the choice of the basis set, select structures were also computed with the GGA of Perdew, Burke, and Ernzerhof (PBE) with the 6-311G** basis set. No effect on the resulting structure was found.

Syntheses

Monomer synthesis

5-bromo-2-hydroxylisophthalaldehyde (Duff reaction) (DAl-OH/Br)

Bromophenol (1.00 eq.), hexamethylentetramine (8.00 eq.) and trifluoracetic acid ($c_{Bromophenol} = 0.34$ mol/L) were introduced into a round-bottom flask equipped with a condenser and a stirring bar. Under continuous stirring, the reaction mixture was heated up to 110 °C. After 48 h the reaction mixture was cooled down to room temperature. The same volume of 4 M hydrochloric acid compared to the volume of trifluoracetic acid (TFA) was added to the reaction mixture and stirred for further 5 h. The resulting solid was filtered off, washed six times with water and dissolved in DCM. The solvent was removed, yielding the desired product as a yellow crystal.

^{1}H-NMR ($CDCl_3$, 300 MHz): δ = 8.06 (s, 2H, *H*C_{Ar}), 10.19 (s, 2H, –(CO)*H*), 11.54 (s, 1H, –O*H*) ppm; **^{13}C-NMR (CDCl3, 75 MHz):** δ = 112.31 (–C_{Ar}Br), 124.79 (–C_{Ar}–), 139.89 (–C_{Ar}H–), 162.41 (–C_{Ar}O–), 190.87 (C=O) ppm; **HRMS (FAB):** $C_8H_5BrO_3$ $[M]^+$ *m/z*: calcd. 228.9495 found 228.9493. Yield: 57%.

General procedure for the alkylation of 5-bromo-2-hydroxylisophthalaldehyde via Williamson ether synthesis

5-bromo-2-hydroxylisophthalaldehyde (1.00 eq.) was introduced into a round-bottom flask equipped with condenser and stirring bar and suspended with potassium carbonate (1.25 eq.) in DMF (c = 0.098 mol/L). Then, the corresponding alkyl halide (1.25 eq.) was added and heated up to 70 °C for 6 h. For introduction of methyl, propyl and octyl groups, methyl, propyl and octyl iodides were used respectively. After cooling down to room temperature, the reaction mixture was washed with brine and extracted three times with

ethyl acetate. The combined organic phases were washed with brine three times and dried over sodium sulfate. The solvent was removed in vacuo and the desired product was obtained.

1-methoxy-4-tert-butyl-2,6-diformylbenzene (DAl-OMe/^{tert}Bu) ^{1}H-NMR (DMSO-d$_6$, 300 MHz): δ = 10.32 (s, 2H, (CO)H), 8.08 (s, 2H, $C_{Ar}H$), 4.03 (s, 3H, –OCH_3), 1.32 (s, 9H, -CH_3) ppm. Yield: 88%.

5-bromo-2-methoxylisophthalaldehyde (DAl-OMe/Br) ^{1}H-NMR (CDCl$_3$, 300 MHz): δ = 10.35 (s, 2H, –(CO)*H*), 8.20 (s, 2H, CH_{Ar}), 4.09 (s, 1H, –OCH_3) ppm; **^{13}C-NMR (CDCl$_3$, 75 MHz):** δ = 67.12 (–OCH_2), 118.73 (–C_{Ar}Br), 131.71 (–C_{Ar}–), 137.69 (–C_{Ar}H–), 164.22 (–C_{Ar}O–), 187.17 (C=O) ppm; **HRMS (FAB):** $C_9H_7BrO_3$ $[M]^+$ *m/z*: calcd. 241.9573 found 241.9572. Yield: 70%. The product was obtained as **yellow crystals**.

5-bromo-2-propoxylisophthalaldehyde (DAl-OPr/Br) ^{1}H-NMR (CDCl$_3$, 300 MHz): δ = 10.34 (s, 2H, –(CO)*H*), 8.19 (s, 2H, CH_{Ar}), 4.08 (t, J = 6.6 Hz, 2H, –OCH_2–), 1.93 (d, J = 7.3 Hz, 2H, –CH_2–), 1.09 (t, J = 7.4 Hz, 3H, –CH_3)ppm; **^{13}C-NMR (CDCl$_3$, 75 MHz):** δ = 10.29 (–*C*H$_3$), 23.21 (–*C*H$_2$–), 82.38 (–O*C*H$_2$–), 118.33 (–C_{Ar}Br), 131.74 (–C_{Ar}–), 137.26 (–C_{Ar}H–), 163.37 (–C_{Ar}O–), 187.15 (*C*=O) ppm; **HRMS (FAB):** $C_{11}H_{11}BrO_3$ $[M]^+$ *m/z*: calcd. 269.9886 found 269.9888. Yield: 61%. The product was obtained as **slightly yellow crystals**.

5-bromo-2-(octyloxy)isophthalaldehyde (DAl-OOct/Br) ^{1}H-NMR (CDCl$_3$, 300 MHz): δ = 10.28 (s, 2H, –(CO)*H*), 8.11 (s, 2H, CH_{Ar}), 4.02–4.16 (m, 2H, –OCH_2–), 1.78–1.94 (m, 2H, –OCH$_2$CH$_2$–), 1.13–1.53 (m, 10H, –(CH$_2$)$_5$–), 0.78–0.92 (m, 3H, –CH$_3$) ppm; **^{13}C-NMR (CDCl$_3$, 75 MHz):** δ = 14.16 (–*C*H$_3$), 22.70 (–*C*H$_2$–), 25.95 (–*C*H$_2$–), 29.28 (–*C*H$_2$–), 29.44 (–*C*H$_2$–), 30.04 (–*C*H$_2$–), 31.87 (–OCH$_2$*C*H$_2$–), 81.25 (–O*C*H$_2$–), 118.47 (–C_{Ar}Br), 131.90 (–C_{Ar}–), 137.40 (–C_{Ar}H–), 163.58 (–C_{Ar}O–), 187.33 (*C*=O) ppm; **HRMS (FAB):** $C_{16}H_{21}BrO_3$ $[M+H]^+$ *m/z*: calcd. 341.0747 found 341.0748. Yield: 31%. The product was obtained as **beige solid**.

General procedure for the Suzuki coupling

The adequate compound (1.00 eq.), potassium vinyltrifluorborate (5.00 eq.), cesium carbonate (3.00 eq.), [1,1′-Bis(diphenylphosphino)ferrocene] dichloropalladium(II), complex with dichloromethane (0.05 eq.) and *p*-benzoquinone (0.05 eq.) were introduced into a microwave vial. A mixture of THF/water (9:1) was added as solvent with a concentration of 0.048 mmol/mL. The reaction mixture was heated up to 100 °C in a microwave reactor for 1 h for the dialdehydes and 2 h for the iodonitrobenzol. Then, the reaction mixture was washed with water and extracted five times with diethyl ether. The combined organic phases were washed with diluted hydrochlorid acid, brine and dried over sodium sulfate. The solvent was removed in vacuo. The raw material was purified by column chromatography (cyclohexane:ethyl acetate = 4:1) in order to obtain the desired product.

2-methoxy-5-vinylisophthalaldehyde (DAl-OMe/Vinyl) ^{1}H-NMR (CDCl$_3$, 300 MHz): δ = 10.40 (t, J = 10.7 Hz, 2H, –(CO)*H*), 8.11 (d, J = 20.5, 2H, CH_{Ar}), 6.71 (dd, J = 17.6, 10.9 Hz, 1H, C_{Ar}C*H*CH$_2$), 5.87 (d, J = 17.6, 1H, C_{Ar}CHCH_2), 5.41 (d, J = 10.8, 1H, C_{Ar}CHCH_2), 4.07 (s, 3H, –OCH_3) ppm; **^{13}C-NMR (CDCl$_3$, 75 MHz):** δ = 66.90 (–O*C*H$_3$), 116.79 (–CH=*C*H$_2$), 130.13 (–C(=O)C_{Ar}), 132.35 (–C_{Ar}H–), 134.23 (–*C*H=CH$_2$), 134.78 (C_{Ar}), 164.81 (–C_{Ar}O–) 188.51 (*C*=O), ppm; **HRMS (FAB):** $C_{11}H_{10}O_3$ $[M]^+$ *m/z*: calcd. 190.0624 found 190.0624. Yield: 73%. The product was obtained as **white solid**.

2-propoxy-5-vinylisophthalaldehyde (DAl-OPr/Vinyl) ^{1}H-NMR (CDCl$_3$, 300 MHz): δ = 10.41 (s, 2H, –(CO)*H*), 8.12 (s, 2H, CH_{Ar}), 6.72 (dd, J = 17.6, 10.9 Hz, 1H, C_{Ar}C*H*CH$_2$), 5.85 (d, J = 17.6, 1H, C_{Ar}CHCH_2), 5.46–5.31 (m, 1H, C_{Ar}CHCH_2), 4.09 (t, J = 6.6 Hz, 2H, –OCH_2–), 2.03–1.85 (m, 2H, –CH_2–), 1.10 (t, J = 7.4 Hz, 3H, –CH_3) ppm; **^{13}C-NMR (CDCl$_3$, 75 MHz):** δ = 10.47 (–*C*H$_3$), 23.38 (–*C*H$_2$–), 82.24 (–O*C*H$_2$–), 116.65 (–CH=*C*H$_2$), 130.32 (C(=O)C_{Ar}), 132.11 (–C_{Ar}H–), 134.31 (*C*H=CH$_2$), 134.55 (C_{Ar}), 164.17 (–C_{Ar}O–), 188.70 (*C*=O) ppm; **HRMS (FAB):** $C_{13}H_{14}O_3$ $[M]^+$ *m/z*: calcd. 218.0937 found 218.0939. Yield: 72%. The product was obtained as **yellow solid**.

2-(octyloxy)-5-vinylisophthalaldehyde (DAl-OOct-Vinyl) ^{1}H-NMR (CDCl$_3$, 300 MHz): δ = 10.39 (s, 2H, –(CO)*H*), 8.10 (s, 2H, CH_{Ar}), 6.71 (ddd, J = 15.9, 10.9, 5.0 Hz, 1H, C_{Ar}C*H*CH$_2$), 5.83 (dd, J = 17.6, 5.0 Hz, 1H, C_{Ar}CHCH_2), 5.38 (dd, J = 10.9, 5.0 Hz, 1H, C_{Ar}CHCH_2), 4.14–4.06 (m, 2H, –OCH_2–), 1.95–1.81 (m, 2H, –OCH$_2$CH_2–), 1.36 (dt, J = 20.5, 9.2 Hz, 10H, –CH_2–), 0.90 (t, J = 12.9 Hz, 3H, –CH_3) ppm; **^{13}C-NMR (CDCl$_3$, 75 MHz):** δ = 14.18 (–*C*H$_3$), 22.73 (–*C*H$_2$-), 25.97 (–*C*H$_2$–), 29.27 (–*C*H$_2$–), 29.44 (–*C*H$_2$–), 30.05 (–OCH$_2$*C*H$_2$–), 31.85 (–*C*H$_2$–), 80.90 (–O*C*H$_2$–), 116.60 (–CH=*C*H$_2$), 130.31 (C(=O)C_{Ar}), 132.07 (–C_{Ar}H–), 134.31 (*C*H=CH$_2$), 134.50 (C_{Ar}), 164.20 (–C_{Ar}O–), 188.67 (*C*=O) ppm; **HRMS (FAB):** $C_{18}H_{24}O_3$ $[M]^+$ *m/z*: calcd. 288.1725 found 288.1719. Yield: 61%. The product was obtained as **yellow solid**.

1,3-dinitro-5-vinylbenzene (DAm-Vinyl) ^{1}H-NMR (CDCl$_3$, 300 MHz): δ = 5.67 (d, J = 10.9 Hz, 1H, –CH=CH_2), 6.08 (d, J = 17.5, 1H, –CH=CH_2), 6.85 (dd,

J = 17.5; 10.9 Hz, 1H, –C*H*=CH_2), 8.56 (d, J = 2.0 Hz, 1H), 8.93 (t, J = 2.0 Hz, 1H, CH_{Ar}) ppm; **^{13}C-NMR ($CDCl_3$, 75 MHz):** δ = 117.52 (–C_{Ar}H), 120.48 (–CH=CH_2), 126.01 (–C_{Ar}H), 133.11 (*C*H=CH_2), 141.33 (C_{Ar}CH=–), 148.92 ($C_{Ar}NO_2$) ppm; **HRMS (GC–MS)** $C_8H_6N_2O_4$ $[–H]^+$ *m/z*: calcd. 194.0328 found 193.6653. Yield: 85%. The product was obtained as **beige solid**.

Synthesis of 1,3-dinitro-5-vinylbenzene by reduction (DAm-Vinyl) Ethanol (c = 0.092 mol/L) was poured and degassed for 10 min with argon in a round-bottom flask equipped with a stirring bar and a condenser closed with septum. 1,3-dinitro-5-vinylbenzene and $SnCl_2$ were added under an argon flow. The reaction mixture was stirred at 95 °C for 4 h. Afterwards, the conversion was checked by ^{1}H-NMR spectroscopy, and if necessary, further $SnCl_2$ was added and the reaction time extended in order to reach full conversion. Then, the solvent was removed in vacuo. The residue was washed with water. The aqueous phase was basified with KOH and extracted three times with diethyl ether. The combined organic phases were washed once with water. After drying the organic phase over sodium sulphate and removing the solvent in vacuo the desired compound was obtained. The product was stored under Ar and in the fridge.

^{1}H-NMR (*d*-acetone, 300 MHz): δ = 4.69 (s, 4H, –NH_2), 5.03 (dd, J = 10.8, 1H, 1.2 Hz, –CH=CH_2), 5.49 (dd, J = 17.6, 1H, –CH=CH_2), 5.77 (t, J = 1.9 Hz, 1H, –CH_{Ar}), 5.91 (t, J = 4.9 Hz, 2H, –CH_{Ar}), 6.40 (dd, J = 17.6, 10.8 Hz, 1H, –C*H*=CH_2) ppm; **^{13}C-NMR (*d*-THF, 75 MHz):** δ = 100.20 (–C_{Ar}H), 101.59 (–C_{Ar}H), 111.60 (–CH=CH_2), 137.76 (*C*H=CH_2), 137.90 (C_{Ar}CH = CH_2), 148.73 ($C_{Ar}NH_2$) ppm; HRMS (GC–MS): $C_8H_{10}N_2$ $[–H]^+$ *m/z*: calcd. 134.1 found 134.1. Yield: 90%. The product was obtained as red highly viscous liquid.

Synthesis of 5-ethylbenzene-1,3-diamine by hydrogenation (DAm-Ethyl)

Iodonitrobenzol (1.00 eq), 10 mg palladium on activated charcoal (10% Pd basis) per 0.1 mmol of starting material and toluene (c = 0.05 mol/L) were introduced into a vessel, equipped with a stirring bar. In a high-pressure reactor, an ethylene pressure of 45 bar was applied. The reaction was stirred for 4 h at room temperature. The progress of the conversion was checked by GC–MS. Afterwards, the turbid reaction mixture was filtered-off and washed with toluene for several times. The solvent was removed in vacuo and the desired product was obtained, and stored under argon in the fridge to prevent a degradation.

^{1}H-NMR (*d*-Benzene, 300 MHz): δ = 1.18 (t, *J* = 7.6 Hz, 3H, –CH_3), 2.44 (q, *J* = 7.6 Hz, 2H, –CH_3–), 2.94 (s, 4H, –NH_2), 5.48 (s, 1H, –$C_{Ar}H$), 5.81 (s, 2H, –$C_{Ar}H$) ppm; **^{13}C-NMR (*d*- Benzene, 75 MHz):** δ = 15.94 (–*C*H_3), 29.48 (–*C*H_2–), 99.81 (–C_{Ar}H), 105.61 (–C_{Ar}H), 146.23 (–C_{Ar}Ethyl), 148.21 ($C_{Ar}NO_2$) ppm; **HRMS (GC–MS):** $C_8H_{12}N_2$ $[–H]^+$ *m/z*: calcd. 135.1 found 135.2. Yield: 92%. The product was obtained as **red highly-viscous liquid**.

Synthesis of macrocycles

General procedure of macrocyclization by imine condensation

A three-neck round-bottom flask was equipped with a stirring bar and a condenser. The system was closed with three septa and via a needle a balloon was attached. Methanol ($c_{Dialdehyde}$ = 0.006 mol/L) was added to the flask and the system closed. The solvent was degassed with Argon for 10 min. In Ar reverse flow, the dialdehyde (1.00 eq.), the diamine (1.00 eq.) and $CaCl_2$ (1.00 eq.) were added. The reaction was heated up to 80 °C and stirred continuously for the respective time. The formed precipitate was collected by centrifugation and decantation of the overlaying solution. By this procedure, the precipitate was washed with methanol until the washed solution was colorless, and dried at high vacuum.

General procedure of reduction of macrocycles

The precipitate was suspended in a mixture of methanol/THF (1:1) ($c_{precipitate}$ = 0.079 mol/L) and $NaBH_4$ (20.0 eq.) was added. The reaction mixture was stirred at room temperature for at least 4 h at which further $NaBH_4$ was added after 2 h. If all precipitate became soluble and the reaction suspension turned into a clear solution, the reaction was quenched by the addition of water. Otherwise, the reaction time was extended and further $NaBH_4$ was added. Subsequently, the reaction mixture was extracted with chloroform three times. The combined organic phases were washed with water one time, dried over sodium sulphate and the solvent was removed in vacuo. The residue was characterized by ^{1}H-NMR spectroscopy, SEC and SEC–ESI.

Macrocycles library

OMe-MC-^{tert}Bu/H ^{1}H-NMR (Benzene-d_6, 300 MHz): δ/ppm = 1.38 (s, 27H, CH_3), 3.61 (s, 9H, O–CH_3), 7.20 (s, 3H, $C_{ar}H$), 7.33–7.38 (t, 3H, $C_{ar}H$), 7.60–7.63 (d, 6H, $C_{ar}H$)), 8.91 (s, 6H, $C_{ar}H$), 9.20 (s, 6H, C*H*=N); Yield: 39.9 mg, 50% (with $CaCl_2$).

OMe-MC-^{tert}Bu/H red ^{1}H-NMR (Benzene-d_6, 300 MHz): δ/ppm = 1.16 (s, 27H, CH_3), 3.63 (s, 9H, O–CH_3), 4.04–4.23 (d, 12H, CH_2), 5.50–5.58 (t, 3H, N*H*), 5.80 (s, 3H, $C_{ar}H$), 5.90–6.05 (d, 6H, $C_{ar}H$)), 6.70–6.82 (t, 3H, $C_{ar}H$), 7.25 (s, 6H, $C_{ar}H$); **^{13}C-NMR (Benzene-d_6, 75 MHz):**

δ = 31.17 (–CH_3 *tert*-butyl), 33.93 (–C– *tert*-butyl), 41.63 (–CH_2), 61.10 (–OCH_3), 95.31 (–C_{Ar}H), 102.07 (–C_{Ar}H), 124.59 (–C_{Ar}H), 128.87 (–C_{Ar}), 131.78 (–C_{Ar}H), 145.53 (–C_{Ar}H), 149.73 (–C_{Ar}H), 153.45 (–C_{Ar}H) ppm.

OH-MC-Br/Vinyl ^{1}H-NMR (THF-d_8, 300 MHz): δ/ppm = 4.14 (s, 12H, –CH_2NH–), 4.79 (s, 6H, –N*H*–), 5.04 (dd, *J* = 10.8, 1.2 Hz, 3H, H_2C=CH–) 5.53 (dd, *J* = 17.6, 1.2 Hz, 3H, H_2C=CH–), 5.82 (s, 3H, *H*C_{Ar}), 6.17 (s, 6H, *H*C_{Ar}), 6.45 (dd, *J* = 17.6, 10.9 Hz, 3H H_2C=C*H*–), 7.12 (s, 6H, *H*C_{Ar}); **HRMS (SEC–ESI):** $C_{48}H_{45}Br_3N_6O_3$ *m/z*($M^- + H^+$) = 991.1172; *m/z*$_{calc.}$ = 991,1181; Δ*m/z* = 0.0009).

OMe-MC-Vinyl/Vinyl ^{1}H-NMR ($CDCl_3$, 300 MHz): δ/ppm = 3.84 – 3.65 (m, 3H, –OCH_3), 4.27 (s, 12H, –CH_2NH–), 4.70 (dd, *J* = 16.9, 11.1 Hz, 6H, –N*H*–), 5.16 (td, *J* = 9.7, 8.8, 4.2 Hz, 6H, H_2C=CH–), 5.83–5.54 (m, 9H, H_2C=CH– & *H*C_{Ar}), 6.18 (dt, *J* = 8.0, 2.0 Hz, 6H, *H*C_{Ar}), 6.72–6.47 (m, 6H, H_2C=C*H*–), 7.35 (d, *J* = 23.7 Hz, 6H, *H*C_{Ar}); **HRMS (SEC–ESI):** $C_{57}H_{60}N_6O_3$ *m/z*($M^- + H^+$) = 877.4770; *m/z*$_{calc.}$ = 877.4805; Δ*m/z* = 0.0035).

OPr-MC-Vinyl/Vinyl HRMS (SEC–ESI): $C_{57}H_{60}N_6O_3$ *m/z*($M^- + H^+$) = 961.5719; *m/z*$_{calc.}$ = 961.5744; Δ*m/z* = 0.0025); $C_{42}H_{48}N_4O_3$ (*m/z*($M^- + H^+$) = 657.3790; *m/z*$_{calc.}$ = 657.3804; Δ*m/z* = 0.0014); $C_{55}H_{62}N_4O_5$ *m/z*($M^- + H^+$) = 859.4774; *m/z*$_{calc.}$ = 859.4798; Δ*m/z* = 0.0024); $C_{63}H_{72}N_6O_4$ *m/z*($M^- + H^+$) = 977.5679; *m/z*$_{calc.}$ = 977.5693; Δ*m/z* = 0.0014); $C_{76}H_{86}N_6O_6$ *m/z*($M^- + H^+$) = 1179.6670; *m/z*$_{calc.}$ = 1179.6687; Δ*m/z* = 0.0017; $C_{84}H_{96}N_8O_5$ *m/z*($M^- + H^+$) = 1297.7556; *m/z*$_{calc.}$ = 1297.7582; Δ*m/z* = 0.0026.

OMe-MC-Br/Vinyl HRMS (SEC–ESI): $C_{57}H_{60}N_6O_3$ *m/z*($M^- + H^+$) = 1055.1249; *m/z*$_{calc.}$ = 1055.1471; Δ*m/z* = 0.0222).

OH-MC-Br/Ethyl HRMS (SEC–ESI): $C_{48}H_{51}Br_3N_6O_3$ *m/z*($M^- + H^+$) = 997.1640; *m/z*$_{calc.}$ = 997.1651; *m/z* = 0.0011).

OMe-MC-Br/Ethyl HRMS (SEC–ESI): $C_{51}H_{57}Br_3N_6O_3$ *m/z*($M^- + H^+$) = 1039.1920; *m/z*$_{calc.}$ = 1039.212; *m/z* = 0.02).

OH-MC-Br/CF_3 ^{1}H-NMR (THF-d_8, 300 MHz): δ/ppm = 4.26 (s, 12H, –CH_2NH–), 5.57 (m, 6H, *H*C_{Ar}), 5.97 (s, 3H, *H*C_{Ar}), 6.36 (6H, –N*H*–), 7.27 (m, 6H, *H*C_{Ar}), 8.59 (s, 3H, O*H*); **HRMS (SEC–ESI):** $C_{45}H_{36}Br_3F_9N_6O_3$ *m/z*($M^- + H^+$) = 1117.0319; *m/z*$_{calc.}$ = 1117.0333; *m/z* = 0.0014.

Acknowlegdements Christopher Barner-Kowollik is acknowledges a Laureate Fellowship from the Australian Research Council (ARC) and continued key support from the Queensland University of Technology (QUT). The authors would like to thank T. Sattelberger, C. Albrecht and T. Anh for experimental support.

References

1. Iyoda, M., Shimizu, H.: Multifunctional π-expanded oligothiophene macrocycles. Chem. Soc. Rev. (2015). https://doi.org/10.1039/c5cs00388a
2. Das, B., McPherson, J.N., Colbran, S.B.: Oligomers and macrocycles with [m] pyridine [n] pyrrole (m + n ≥ 3) domains: formation and applications of anion, guest molecule and metal ion complexes. Coord. Chem. Rev. (2018). https://doi.org/10.1016/j.ccr.2018.02.015
3. Hger, S.: Highly efficient methods for the preparation of shape-persistent macrocyclics. J. Polym. Sci. A (1999). https://doi.org/10.1002/(sici)1099-0518(19990801)37:15%3c2685:aid-pola1%3e3.0.co;2-s
4. Höger, S.: Shape-persistent macrocycles: from molecules to materials. Chemistry (Weinheim an der Bergstrasse, Germany) (2004). https://doi.org/10.1002/chem.200305496
5. Iyoda, M., Yamakawa, J., Rahman, M.J.: Conjugated macrocycles: concepts and applications. Angew. Chem. Int. Ed. Engl. (2011). https://doi.org/10.1002/anie.201006198
6. Naddo, T., Che, Y., Zhang, W., Balakrishnan, K., Yang, X., Yen, M., Zhao, J., Moore, J.S., Zang, L.: Detection of explosives with a fluorescent nanofibril film. J. Am. Chem. Soc. (2007). https://doi.org/10.1021/ja070747q
7. Du, Y., Yang, H., Wan, S., Jin, Y., Zhang, W.: A titanium-based porous coordination polymer as a catalyst for chemical fixation of CO_2. J. Mater. Chem. A (2017). https://doi.org/10.1039/c7ta01188a
8. Hu, X., Yu, C., D Okochi, K., Jin, Y., Liu, Z., Zhang, W.: Phenylene vinylene macrocycles as artificial transmembrane transporters. Chem. Commun. (Camb.) (2016). https://doi.org/10.1039/c6cc01657j
9. Zhang, W., Moore, J.S.: Shape-persistent macrocycles: structures and synthetic approaches from arylene and ethynylene building blocks. ChemInform (2006). https://doi.org/10.1002/chin.200641239
10. Lehn, J.-M.: From supramolecular chemistry towards constitutional dynamic chemistry and adaptive chemistry. ChemInform (2007). https://doi.org/10.1002/chin.200720232
11. Jin, Y., Yu, C., Denman, R.J., Zhang, W.: Recent advances in dynamic covalent chemistry. Chem. Soc. Rev. (2013). https://doi.org/10.1039/c3cs60044k
12. Rowan, S.J., Cantrill, S.J., Cousins, G.R.L., Sanders, J.K.M., Stoddart, J.F.: Dynamic covalent chemistry. Angew. Chem. Int. Ed. (2002). https://doi.org/10.1002/1521-3773(20020503)41:9%3c1460:aid-anie11111460%3e3.0.co;2-n
13. Jin, Y., Wang, Q., Taynton, P., Zhang, W.: Dynamic covalent chemistry approaches toward macrocycles, molecular cages, and polymers. Acc. Chem. Res. (2014). https://doi.org/10.1021/ar500037v
14. Ge, P.-H., Fu, W., Herrmann, W.A., Herdtweck, E., Campana, C., Adams, R.D., Bunz, U.H.F.: Structural characterization of a cyclohexamericmeta-phenyleneethynylene made by alkyne metathesis with in situ catalysts. Angew. Chem. (2000). https://doi.org/10.1002/1521-3757(20001016)112:20%3c3753:aid-ange3753%3e3.0.co;2-b

15. Zhang, W., Moore, J.S.: Arylene ethynylene macrocycles prepared by precipitation-driven alkyne metathesis. J. Am. Chem. Soc. (2004). https://doi.org/10.1021/ja046531v
16. Heppekausen, J., Stade, R., Goddard, R., Fürstner, A.: Practical new silyloxy-based alkyne metathesis catalysts with optimized activity and selectivity profiles. J. Am. Chem. Soc. (2010). https://doi.org/10.1021/ja104800w
17. Yang, H., Liu, Z., Zhang, W.: Multidentate triphenolsilane-based alkyne metathesis catalysts. Adv. Synth. Catal. (2013). https://doi.org/10.1002/adsc.201201105
18. Zhao, D., Moore, J.S.: Synthesis and self-association of an imine-containing m-phenylene ethynylene macrocycle. J. Org. Chem. (2002). https://doi.org/10.1021/jo010918o
19. Jin, Y., Zhang, A., Huang, Y., Zhang, W.: Shape-persistent arylenevinylene macrocycles (AVMs) prepared via acyclic diene metathesis macrocyclization (ADMAC). Chem. Commun. (Camb.) (2010). https://doi.org/10.1039/c0cc02941f
20. Hartley, C.S., Moore, J.S.: Programmed dynamic covalent assembly of unsymmetrical macrocycles. J. Am. Chem. Soc. (2007). https://doi.org/10.1021/ja0745963
21. Okochi, K.D., Jin, Y., Zhang, W.: Highly efficient one-pot synthesis of hetero-sequenced shape-persistent macrocycles through orthogonal dynamic covalent chemistry (ODCC). Chem. Commun. (Camb.) (2013). https://doi.org/10.1039/c2cc33078d
22. Meyer, C.D., Joiner, C.S., Stoddart, J.F.: Template-directed synthesis employing reversible imine bond formation. Chem. Soc. Rev. (2007). https://doi.org/10.1039/b513441m
23. Melson, G.A., Busch, D.H.: Reactions of coordinated ligands. X. The formation and properties of a tetradentate macrocyclic ligand by the self-condensation of o-aminobenzaldehyde in the presence of metal ions. J. Am. Chem. Soc. (1964). https://doi.org/10.1021/ja01076a022
24. Storm, O., Lüning, U.: How to synthesize macrocycles efficiently by using virtual combinatorial libraries. Chemistry (Weinheim an der Bergstrasse, Germany) (2002). https://doi.org/10.1002/1521-3765(20020215)8:4%3c793:aid-chem793%3e3.0.co;2-u
25. Höger, S.: Shape-persistent rings and wheels. Pure Appl. Chem. (2010). https://doi.org/10.1351/PAC-CON-09-09-01
26. MacLachlan, M.J.: conjugated shape-persistent macrocycles via schiff base condensation: new motifs for supramolecular chemistry. ChemInform (2006). https://doi.org/10.1002/chin.200628264
27. Shopsowitz, K.E., Edwards, D., Gallant, A.J., MacLachlan, M.J.: Highly substituted Schiff base macrocycles via hexasubstituted benzene: a convenient double Duff formylation of catechol derivatives. Tetrahedron (2009). https://doi.org/10.1016/j.tet.2009.07.094
28. Ferguson, J.S., Yamato, K., Liu, R., He, L., Zeng, X.C., Gong, B.: One-pot formation of large macrocycles with modifiable peripheries and internal cavities. Angew. Chem. (2009). https://doi.org/10.1002/ange.200900584
29. Akine, S., Taniguchi, T., Nabeshima, T.: Synthesis and crystal structure of a novel triangular macrocyclic molecule, tris(H 2 saloph), † †H2saloph = N, N′-disalicylidene-o-phenylenediamine and its water complex. Tetrahedron Lett. (2001). https://doi.org/10.1016/s0040-4039(01)01943-8
30. Gallant, A.J., Hui, J.K.-H., Zahariev, F.E., Wang, Y.A., MacLachlan, M.J.: Synthesis, structure, and computational studies of soluble conjugated multidentate macrocycles. J. Org. Chem. (2005). https://doi.org/10.1021/jo050742g
31. Reinhard, D., Schöttner, L., Brosius, V., Rominger, F., Mastalerz, M.: Synthesis of para-aryl-substituted salicyldialdehydes. Eur. J. Org. Chem. (2015). https://doi.org/10.1002/ejoc.201500228
32. Duff, J.C., Bills, E.J.: 273 Reactions between hexamethylenetetramine and phenolic compounds. Part I. A new method for the preparation of 3- and 5-aldehydosalicylic acids. J. Chem. Soc. (1932). https://doi.org/10.1039/JR9320001987
33. Brooker, M.D., Cooper, S.M., Hodges, D.R., Carter, R.R., Wyatt, J.K.: Studies of microwave-enhanced Suzuki-Miyaura vinylation of electron-rich sterically hindered substrates utilizing potassium vinyltrifluoroborate. Tetrahedron Lett. (2010). https://doi.org/10.1016/j.tetlet.2010.10.087
34. Akine, S., Hashimoto, D., Saiki, T., Nabeshima, T.: Synthesis and structure of polyhydroxyl rigid triangular nano-macrocyclic imine having multiple hydrogen-bonding sites. Tetrahedron Lett. (2004). https://doi.org/10.1016/j.tetlet.2004.04.015
35. Houjou, H., Lee, S.-K., Hishikawa, Y., Nagawa, Y., Hiratani, K.: Highly selective formation of 2:2 macrocycles from a novel hydroxybenzaldehyde derivative and diamines. Chem. Commun. (2000). https://doi.org/10.1039/b005536k
36. Terao, J., Nakamura, M., Kambe, N.: Non-catalytic conversion of C-F bonds of benzotrifluorides to C-C bonds using organoaluminium reagents. Chem. Commun. (Camb.) (2009). https://doi.org/10.1039/b915620h
37. Fave, G.M.L.: Some reactions of the trifluoromethyl group in the benzotrifluoride series. I. Hydrolysis. J. Am. Chem. Soc. (1949). https://doi.org/10.1021/ja01180a507
38. Scheurer, P.G., Le Fave, G.M.: Isophthalic and terephthalic acids 1. J. Am. Chem. Soc. (1950). https://doi.org/10.1021/ja01163a539
39. Zhu, J., Pérez, M., Caputo, C.B., Stephan, D.W.: Use of trifluoromethyl groups for catalytic benzylation and alkylation with subsequent hydrodefluorination. Angew. Chem. (2016). https://doi.org/10.1002/ange.201510494
40. Kempe, K., Krieg, A., Becer, C.R., Schubert, U.S.: "Clicking" on/with polymers: a rapidly expanding field for the straightforward preparation of novel macromolecular architectures. Chem. Soc. Rev. (2012). https://doi.org/10.1039/c1cs15107j
41. Lammens, M., Fournier, D., Fijten, M.W.M., Hoogenboom, R., Du Prez, F.: Star-shaped polyacrylates: highly functionalized architectures via CuAAC click conjugation. Macromol. Rapid Commun. (2009). https://doi.org/10.1002/marc.200900494
42. Khuong, K.S., Jones, W.H., Pryor, W.A., Houk, K.N.: The mechanism of the self-initiated thermal polymerization of styrene. Theoretical solution of a classic problem. J. Am. Chem. Soc. (2005). https://doi.org/10.1021/ja0448667

Affiliations

Gregor Klein[1,3] · Audrey Llevot[1,2] · Pia Löser[1] · Benjamin Bitterer[1] · Julian Helfferich[4] · Wolfgang Wenzel[4] · Christopher Barner-Kowollik[3] · Michael A. R. Meier[1]

✉ Audrey Llevot
audrey.llevot@enscbp.fr

✉ Michael A. R. Meier
m.a.r.meier@kit.edu
http://www.meier-michael.com

[1] Laboratory of Applied Chemistry, Institute of Organic Chemistry (IOC), Karlsruhe Institute of Technology (KIT), Straße am Forum 7, 76131 Karlsruhe, Germany

[2] Laboratoire de Chimie des Polymères Organiques (LCPO), UMR 5629, University of Bordeaux, CNRS, Bordeaux INP, 16 avenue Pey-Berland, 33607 Pessac Cedex, France

[3] Soft Matter Materials Laboratory, School of Chemistry, Physics and Mechanical Engineering, Queensland University of Technology (QUT), 2 George Street, Brisbane, QLD 4000, Australia

[4] Karlsruhe Institute of Technology (KIT), Institute of Nanotechnology (INT), Karlsruhe Institute of Technology (KIT), 76344 Eggenstein-Leopoldshafen, Germany